# Surfactant-Directed Zeolite Nanosheets: A High-Performance Catalyst for Gas-Phase Beckmann Rearrangement

Jeongnam Kim,[†] Woojin Park,[†,‡] and Ryong Ryoo[*,†,‡]

[†]Center for Functional Nanomaterials and Department of Chemistry and [‡]Graduate School of Nanoscience and Technology (WCU), KAIST, Daejeon 305-701, Republic of Korea

**S** *Supporting Information*

**ABSTRACT:** Silica nanosheets with an MFI zeolite topology having a thickness of 2 nm were synthesized following a synthetic route using $[C_{16}H_{33}-N^+(CH_3)_2-C_6H_{12}-N^+(CH_3)_2-C_6H_{13}](OH^-)_2$ as a zeolite structure-directing agent. The surfactant-directed zeolite nanosheets exhibited a remarkably long catalytic lifetime and high selectivity for the production of $\varepsilon$-caprolactam via gas-phase Beckmann rearrangement of cyclohexanone oxime, as compared with amorphous silica and bulk silica zeolite. The distinct catalytic performance of the nanosheets is attributable to silanol groups located on the surfactant-terminated crystal surfaces.



*Zeolite MFI nanosheets synthesized using 'structure-directing' surfactants*

**KEYWORDS:** zeolite nanosheets, Beckmann rearrangement, oxime, caprolactam, silicalite, hierarchical,
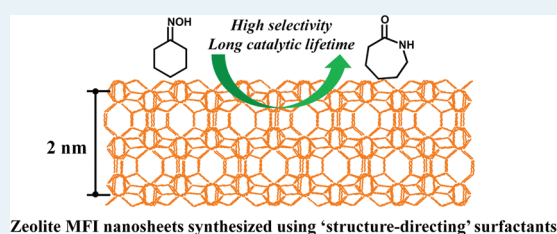
Zeolites are crystalline microporous materials that have found widespread applications in catalysis due to their catalytic activity and structural stability and the well-defined topology of their micropores sized to molecular dimensions (<1 nm).[1] These conventional zeolites are typically synthesized in the presence of alkali metal ions or organic amines as structure-directing agents (SDAs).[2] However, many of the resultants are formed as micrometer-sized bulk crystals (i.e., billions of tiny micropores in a single crystal), often associated with slow mass transfers into and out of the catalytic sites inside the zeolite frameworks. Great efforts have been made to overcome this diffusion limitation by means of reducing the crystal size or generating large mesopores (>2 nm) into the bulk crystal.[3−5] For MCM-22 and ferrierite, it was also possible to prepare nanosheets through a delamination process of the layered precursors. This led to a remarkable improvement in the diffusion.[4,6−8]

Recently, a new synthetic strategy to prepare zeolite with a framework thickness of <5 nm was reported in which a zeolite-SD-group-functionalized organic surfactant was used as the SDA.[9,10] In this approach, the formation of the zeolite structure occurs only at the hydrophilic part of the surfactant while long hydrophobic alkyl tails restrict the crystal growth along a specific direction. One successful synthesis example is an MFI zeolite having a nanosheet-like morphology with a thickness of 2 nm along the *b*-axis, generated by $C_{22}H_{46}-N^+(CH_3)_2-C_6H_{12}-N^+(CH_3)_2-C_6H_{13}$. It is noteworthy that these MFI nanosheets exhibited a tremendously long lifetime during the methanol-to-hydrocarbon catalytic conversion as compared with bulk MFI zeolites.[9,11] This was explained in terms of the facile diffusion of coke precursors from the micropores to the external surfaces owing to an extremely short diffusion path length. Furthermore, a large number of surface acid sites in the nanosheet catalyst made it suitable for the catalytic transformation of bulky molecules,

even when strong acidity is required.[6] We expect that in the coming years, the surfactant-directed synthesis method will be more generally used for other related nanomorphic zeolites; their catalytic properties offer a unique opportunity related to the development of alternative energy sources through green chemical processes.[8,12]

In the present work, we report that a cyclohexanone oxime (CHO)-to-$\varepsilon$-caprolactam (CL, a precursor of Nylon-6) Beckmann rearrangement can be realized with high selectivity and a surprisingly long catalytic lifetime when ultrathin MFI silica nanosheets are used as a gas-phase reaction catalyst. Sumitomo Chemical initially established such a gas-phase heterogeneous catalytic process for the industrial green production of CL via Beckmann rearrangement without using a sulfuric acid catalyst, thereby generating $(NH_4)_2SO_4$ as a byproduct.[13−16] The siliceous MFI catalyst is a key component in this green chemical process for obtaining a high catalytic conversion rate and feasible CL selectivity (Scheme 1).[13−20] However, the catalyst lifetime is still far too short for application to a fixed bed reactor, even if the zeolite is properly treated beforehand with methods such as a $NH_3/NH_4^+$ solution treatment at a pH of 11.[21−24] The nanosheet catalyst used in the present study exhibits remarkable catalytic activity and longevity without any pretreatments. The surfaces of the silica nanosheets are fully covered with silanol groups, providing highly active sites.
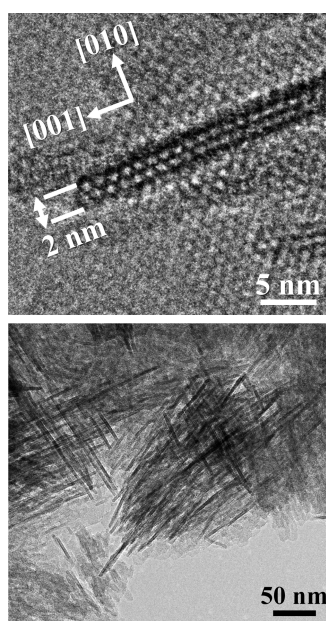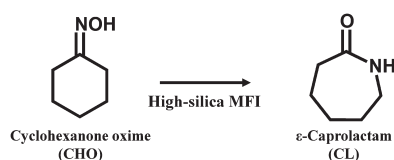
The MFI zeolite nanosheets were hydrothermally synthesized in a siliceous form using $[C_{16}H_{33}-N^+(CH_3)_2-C_6H_{12}-N^+(CH_3)_2-C_6H_{13}](OH^-)_2$ as a zeolite SDA and tetraethoxysilane (TEOS, Junsei, 95%) as a silica source under sodium-free
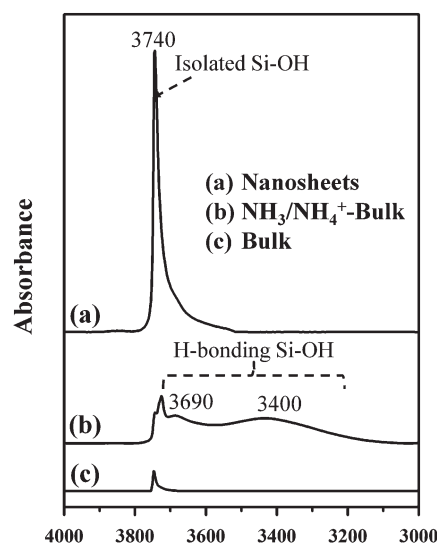
**Scheme 1. Gas Phase Beckmann Rearrangement of CHO to CL over High-Silica MFI Catalysts**



**Figure 1.** TEM images of MFI silica nanosheets with a single-unit-cell thickness along the crystallographic *b*-axis.



**Figure 2.** FT-IR spectra of (a) MFI silica nanosheets, (b) $NH_3/NH_4^+$-treated bulk, and (c) pristine bulk MFI silica samples.

synthesis conditions according to a procedure reported in the literature.[9,10] The zeolite was calcined in air under static conditions at 773 K and then was used as a catalyst in powder form. For comparison, a bulk MFI-silica sample was synthesized using tetrapropylammonium hydroxide (TPAOH) and TEOS. The bulk zeolite was tested as a catalyst after calcination and after an additional treatment in an $NH_3/NH_4^+$ solution at a pH of 11 following the same procedure reported by Kitamura et al.[25] All the catalysts prepared in this work had a sufficiently low Al content so as not to cause catalytic conversion by Al impurities. The Si/Al ratios were >2000 as determined from elemental analysis (Table S1, Supporting Information). Beckmann rearrangement of CHO, 4-methyl-pentane-2-one oxime (MPO), and cyclopentanone oxime (CPO) was carried out over the powder catalyst in a fixed-bed reactor at 623 K in an oxime−ethanol mixture carried by a $N_2$ gas stream.[17,26] The details are described in the Experimental Methods section.

As shown in Figure 1, the MFI zeolite nanosheets are 2.0 nm thick along the *b*-axis dimension of the MFI crystal lattice. This thickness is composed of three pentasil sheets and corresponds to the single-unit-cell dimension ($b$ = 1.9738 nm).[9] Each nanosheet was ∼60 nm wide in the *a*−*c* plane. These nanosheets were obtained as a fully disordered assembly with a large mesopore volume (∼0.8 $cm^3 g^{-1}$) between the nearest neighbors. The BET surface area (640 $m^2 g^{-1}$) is much larger than the BET area of the bulk MFI silica (320 $m^2 g^{-1}$), with the difference

being due to the large external surface area of the former (Table S1 of the Supporting Information). The nanosheet surface contained as many as 2.1 mmol silanol groups per gram of sample. This was determined from the magic-angle-spinning ^{29}Si NMR signal intensity ratio between the Si in a $Q^3$ environment (i.e., tetrahedral Si bonded to three −SiOSi≡ and one −SiOH) and Si in all environments (i.e., $Q^3 + Q^4$) (Figure S1 of the Supporting Information). Nearly all the silanol groups were identified as non-H-bonding silanols (∼3740 $cm^{-1}$) by FT-IR spectroscopy (Figure 2). A negligible amount of H-bonding silanols was detected by IR investigation. Compared with the nanosheet sample, the bulk MFI silica exhibited very low IR spectral intensities (Figure 2). After treatment with a $NH_3/NH_4^+$ solution, other strong adsorption peaks assignable to H-bonding vicinal silanols (∼3690 $cm^{-1}$) and silanol nests (∼3400 $cm^{-1}$) appeared.[17]
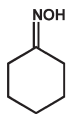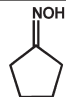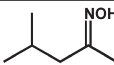
In the presence of the large concentration of non-H-bonding surface silanols, the MFI nanosheets exhibited high catalytic conversion of CHO, high selectivity to CL, and, most significantly, a long catalytic lifetime (Figure 3). As shown in Figure 3, the initial conversion of CHO over the nanosheet catalyst was 84%. The selectivity to CL was 90%, and the catalytic conversion decreased only to 63% after 100 h. Moreover, the selectivity remained unchanged during that period. On the other hand, the bulk catalyst exhibited 66% initial conversion and was deactivated very rapidly to 15% conversion within only 20 h. Furthermore, the CL selectivity never exceeded 6% during the application of the catalyst. The catalytic selectivity of the bulk zeolite was greatly improved to 85−90% after a treatment in $NH_3/NH_4^+$, showing good agreement with a previous report documenting catalytic improvement due to the generation of silanol nests;[17] however, the catalytic lifetime was not improved under the reaction conditions at 623 K.

The long catalytic lifetime of the nanosheets can be explained by the facile removal of coke-generating polymeric species that lead to deactivation of the catalytic sites. This explanation is supported by a significant difference in coke contents between the nanosheet and bulk MFI catalyst (4 and 7 wt %, respectively), which has been determined by thermogravimetric analysis after the same reaction period of 24 h. The effect of facile diffusion on
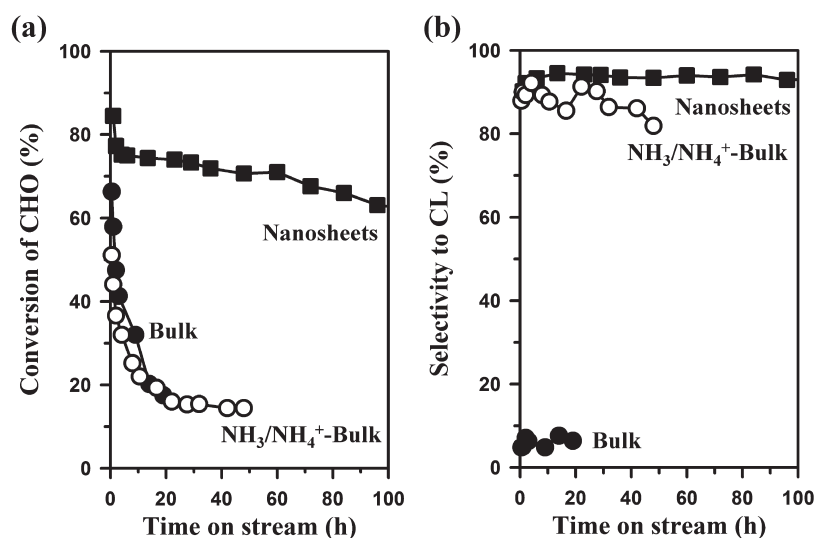
**Figure 3.** Catalytic activity (a) and CL selectivity (b) as a function of the time on-stream during the gas-phase Beckmann rearrangement of CHO into CL over MFI silica catalysts (reaction conditions: 10 wt % oxime in ethanol; WHSV, 3 h$^{-1}$; temp, 623 K).

**Table 1. Catalytic Results for Gas-Phase Beckmann Rearrangement of CHO, CPO, and MPO over Various Silica Catalysts**[a]

| Substrate | Catalyst | Conversion (%) | Selectivity to lactam (%) |
|---|---|---|---|
| | Nanosheets | 77 | 92 (1/0/7)[e] |
| NOH (Cyclohexanone oxime) | Bulk | 48 | 5.0 (2/7/86) |
| | NH$_3$/NH$_4^+$-Bulk | 32 | 92 (2/0/6) |
| | Mesoporous[b] | 49 | 4.7 |
| | Nanoparticles[c] | 25 | 1.0 |
| | KIT-6[d] | 14 | 50 |
| NOH (Cyclopentanone oxime) | Nanosheets | 47 | 82 |
| | Bulk | 30 | 1.0 |
| | NH$_3$/NH$_4^+$-Bulk | 15 | 81 |
| NOH (4-methyl-pentane-2-one oxime) | Nanosheets | 47 | 86 |
| | Bulk | 20 | 55 |
| | NH$_3$/NH$_4^+$-Bulk | 27 | 92 |

[a] Reaction conditions: 10 wt % of oxime in ethanol, WHSV (oxime) = 3 h$^{-1}$, temp = 623 K, time = 2 h. [b] Mesoporous MFI zeolite synthesized using mesoporous carbon as a template. [c] MFI silica nanoparticles synthesized with TPAOH at a low temperature (333 K). [d] Ordered mesoporous silica with cubic $Ia3d$ symmetry. [e] The numbers in parentheses indicate percentage selectivity to cyclohexanone/nitriles/others.

the catalytic lifetime is similar to the effect of mesoporosity on the catalytic conversion of methanol to hydrocarbons.[11] However, the high selectivity to CL is difficult to explain with facile diffusion. We synthesized an MFI silica sample using TPAOH at a low temperature and a mesoporous MFI zeolite using mesoporous carbon as a template.[27-29] The zeolite sample obtained from the low-temperature synthesis was ~50 nm in particle diameters. The carbon-templated zeolite consisted of very thin zeolite frameworks thinner than 10 nm. Despite such small crystallite sizes for facile diffusion, these zeolites still exhibited very poor CL selectivity of less than 5% (Table 1). Thus, the high selectivity of the MFI nanosheet was difficult to attribute to facile diffusion.

It is generally agreed that silanols are the catalytic active site in the CHO-to-CL reaction over silica surfaces.[13-18] Nevertheless, the catalytic activity and CL selectivity markedly depended on the surface structure. The aforementioned 50-nm zeolite nanoparticles and the carbon-templated zeolite possessed high concentrations of surface silanols, but they exhibited poor selectivity (Table 1). MCM-41-type mesoporous silicas were also investigated in this work, but the silanol groups on the noncrystalline frameworks were found to be much less selective than the nanosheet sample (Table 1). Thus, the selectivity seemed to change dramatically, depending on the detailed structure of the silanol arrangement. In particular, the case of MFI nanosheet without ammonia treatment could be attributed to high silanol

content at the external surface because the zeolite structure did not contain other silanols, such as silanol nest, significantly.

Compared with other silica catalysts, the MFI nanosheets had an extremely large portion of (010) crystal lattice planes (i.e., wide $a-c$ planes) among the crystal planes exposed to the surface. This was exclusively due to the zeolite SD caused by the surfactants, which strongly induced anisotropic crystal growth with large (010) planes.[9] This suggests, therefore, that the surface silanols located at the (010) crystal plane are catalytic active sites that exhibit high selectivity to CL with a long catalytic lifetime. On the other hand, the MFI zeolites generated by small TPA cations are anticipated to have other types of surface planes that may lead to poor catalytic performance. Such surface plane dependence of the catalytic property is typical for crystalline metal or metal oxide materials.[30,31] However, unfortunately, it remains unclear how the reactivity and selectivity of the surface silanols is related to the zeolite surface planes. One plausible explanation may be found in the difference in the silanol arrangement and concentration, depending on the MFI crystal surface. Another is that the (010) surface appears to have external pore openings, similar to the surface pockets in the (001) planes of MWW zeolite, providing unusually high selectivity during the catalytic production of cumene.[32,33] As in the previous case, if this exists, the present high selectivity may be explained by the theory of the zeolite confinement effect, termed the "nest effect".[34−36] Further detailed studies are ongoing in our laboratory.

The nanosheet zeolite and bulk catalyst also exhibited significant differences in the gas-phase Beckmann rearrangement of the other oximes of MPO and CPO (Table 1). The nanosheet catalyst was always highly selective for the corresponding lactams (>82%) when MPO and CPO were reacted. On the other hand, the bulk catalyst exhibited very poor selectivity to lactams (55% for MPO and 1% for CPO). After the treatment with the $NH_3/NH_4^+$ solution, the selectivity to both lactams was markedly improved by more than 81%, but the catalytic conversions were at least two times lower than those of the nanosheet catalyst under identical reaction conditions.

It is interesting to note that the nanosheet catalyst showed similar catalytic performance, even after the $NH_3/NH_4^+$ treatment (Figure S2 of the Supporting Information). This result indicates that the generation of silanol nests into the nanosheet frameworks does not play a significant role in the improvement of catalytic activity. Instead, the initial catalytic conversion can be increased to 100% with a CL selectivity of 90% with the increase in the amount of the nanosheet catalyst (i.e., increased contact time). The MFI nanosheet catalyst is also reusable without a significant loss of its initial activity when the coke deposited on the catalyst is burned off by flowing air at 773 K.

In summary, we have demonstrated that an MFI silica nanosheet with a thickness of 2 nm along the $b$-axis is an extraordinarily selective catalyst for the gas-phase Beckmann rearrangement of CHO to CL. In addition to affording high selectivity, the nanosheet catalyst maintains catalytic activity that is more than 10 times longer than the currently industrialized bulk zeolite catalyst under the present reaction conditions. We attribute this remarkable catalytic performance of the nanosheet catalyst to silanol groups located on the external surface of the nanosheet. We believe that these results provide valuable insights into the nature of external catalytic sites of surfactant-directed, nanoscale zeolitic materials.

## EXPERIMENTAL METHODS

**Catalyst Preparation.** MFI silica nanosheets were hydrothermally synthesized using $[C_{16}H_{33}-N^+(CH_3)_2-C_6H_{12}-N^+-(CH_3)_2-C_6H_{13}](OH^-)_2$ [in short, $C_{16-6-6}(OH)_2$] as the SDA following a procedure previously reported by us.[9,10] The experimental procedure is briefly described as follows: 22.8 g of $C_{16-6-6}(OH)_2$ solution (4.5 wt %) was mixed with 4.2 g of TEOS, giving a molar composition of 100 $SiO_2$/10 $C_{16-6-6}(OH)_2$/6000 $H_2O$. The mixture was hand-shaken vigorously for 5 min and then stirred at 333 K for 2 h. Subsequently, the aged mixture was transferred into a Teflon-lined stainless-steel autoclave and heated to 413 K for 5 d while tumbling (60 rpm) in an oven. After hydrothermal crystallization, the zeolite product was filtered, washed with deionized water, and dried at 403 K. The zeolite was calcined in air under static conditions at 773 K. For comparison, a bulk MFI-silica sample was synthesized using TPAOH as the SDA according to a procedure described in the literature.[17] The bulk zeolite was additionally modified with an $NH_3/NH_4^+$ solution at a pH of 11. Typically, 5 g of bulk zeolite was treated with an aqueous solution containing 5 g of ammonia solution (25 wt %) and 15 g of ammonium nitrate solution (7.5 wt %) at 363 K for 2 h under vigorous stirring.[17]

**Catalytic Test.** Gas-phase Beckmann rearrangements of CHO, MPO, and CPO were carried out over a powder catalyst in a fixed-bed quartz reactor (i.d. = 15 mm) at 623 K in an oxime−ethanol mixture (weight ratio 1:9) carried by a $N_2$ gas stream.[17,26] The reaction temperature was measured by a K-type thermocouple inserted into the reactor. Prior to the catalytic reaction, the catalyst was activated at 723 K for 3 h under flowing air (50 mL min$^{-1}$). The feed rate of the oxime−ethanol solution was controlled with a HPLC pump. The weight hourly space velocity (WHSV) was 3 $g_{oxime}$ $g_{cat}^{-1}$ h$^{-1}$. The gaseous effluents were condensed in a glass condenser (273 K), and the liquid products were then collected at regular time intervals. A product analysis was performed with a gas chromatograph (GC, Younglin, Acme-6000) equipped with a flame ionization detector and a capillary column (HP-Innowax, J&W). The products were identified with GC combined with mass spectrometry (Agilent 6890 series).

## ASSOCIATED CONTENT

**ⓢ Supporting Information.** Experimental details and supporting table and figures. This material is available free of charge via the Internet at http://pubs.acs.org/.

## AUTHOR INFORMATION

**Corresponding Author**
*Phone: (+82) 42 350 2830. Fax: (+82) 42 350 8130. E-mail: rryoo@kaist.ac.kr.

## ACKNOWLEDGMENT

## REFERENCES

(1) Corma, A. *Chem. Rev.* **1997**, *97*, 2373–2420.
(2) Cundy, C. S.; Cox, P. A. *Chem. Rev.* **2003**, *103*, 663–702.

(3) Tao, Y.; Kanoh, H.; Abrams, L.; Kaneko, K. *Chem. Rev.* **2006**, *106*, 896–910.

(4) Egeblad, K.; Christensen, C. H.; Kustova, M.; Christensen, C. H. *Chem. Mater.* **2008**, *20*, 946–960.

(5) Pérez-Ramírez, J.; Christensen, C. H.; Egeblad, K.; Christensen, C. H.; Groen, J. C. *Chem. Soc. Rev.* **2008**, *37*, 2530–2542.

(6) Corma, A.; Fornes, V.; Pergher, S. B.; Maesen, Th. L. M.; Buglass, J. G. *Nature* **1998**, *396*, 353–356.

(7) Corma, A.; Fornés, V.; Martínez-Triguero, J.; Pergher, S. B. *J. Catal.* **1999**, *186*, 57–63.

(8) Tsapatsis, M.; Fan, W. *ChemCatChem* **2010**, *2*, 246–248.

(9) Choi, M.; Na, K.; Kim, J.; Sakamoto, Y.; Terasaki, O.; Ryoo, R. *Nature* **2009**, *461*, 246–250.

(10) Na, K.; Choi, M.; Park, W.; Sakamoto, Y.; Terasaki, O.; Ryoo, R. *J. Am. Chem. Soc.* **2010**, *132*, 4169–4177.

(11) Kim, J.; Choi, M.; Ryoo, R. *J. Catal.* **2010**, *269*, 219–228.

(12) Morris, R. E. *Top. Catal.* **2010**, *53*, 1291–1296.

(13) Sato, H. *Catal. Rev. Sci. Eng.* **1997**, *39*, 395–424.

(14) Ichihashi, H.; Kitamura, M. *Catal. Today* **2002**, *73*, 23–28.

(15) Izumi, Y.; Ichihashi, H.; Shimazu, Y.; Kitamura, M.; Sato, H. *Bull. Chem. Soc. Jpn.* **2007**, *80*, 1280–1287.

(16) Dahlhoff, G.; Niederer, P. M.; Hölderich, W. F. *Catal. Rev. Sci. Eng.* **2001**, *43*, 381–441.

(17) Heitmann, G. P.; Dahlhoff, G.; Hölderich, W. F. *J. Catal.* **1999**, *186*, 12–19.

(18) Fernández, A. B.; Marinas, A.; Blasco, T.; Fornés, V.; Corma, A. *J. Catal.* **2006**, *243*, 270–277.

(19) Li, W. C.; Lu, A. H.; Palkovits, R.; Schmidt, W.; Spliethoff, B.; Schüth, F. *J. Am. Chem. Soc.* **2005**, *127*, 12595–12600.

(20) Kath, H.; Gläser, R.; Weitkamp, J. *Chem. Eng. Technol.* **2001**, *24*, 150–153.

(21) Tao, W.; Mao, D.; Xia, J.; Chen, Q.; Hu, Y. *Chem. Lett.* **2005**, *34*, 472–473.

(22) Forni, L.; Fornasari, G.; Giordano, G.; Lucarelli, C.; Katovic, A.; Trifirò, F.; Perri, C.; Nagy, J. B. *Phys. Chem. Chem. Phys.* **2004**, *6*, 1842–1847.

(23) Takahashi, T.; Nasution, M. N. A.; Kai, T. *Appl. Catal., A* **2001**, *210*, 339–344.

(24) Cesana, A.; Palmery, S.; Buzzoni, R.; Spanò, G.; Rivetti, F.; Carnelli, L. *Catal. Today* **2010**, *154*, 264–270.

(25) Kitamura, M.; Ichihashi, H.; Tojima, H. U.S. Patent 5 212 302, 1993.

(26) Yashima, T.; Oka, N.; Komatsu, T. *Catal. Today* **1997**, *38*, 249–253.

(27) Creaser, Q. L. D.; Sterte, J. *Microporous Mesoporous Mater.* **1999**, *31*, 141–150.

(28) Jacobsen, C. J. H.; Madsen, C.; Houzvicka, J.; Schmidt, I.; Carlsson, A. *J. Am. Chem. Soc.* **2000**, *122*, 7116–7177.

(29) Kim, T.-W.; Solovyov, L. A. *J. Mater. Chem.* **2006**, *16*, 1445–1455.

(30) Somorjai, G. A; Frei, H.; Park, J. Y. *J. Am. Chem. Soc.* **2009**, *131*, 16589–16605.

(31) Yang, H. G.; Sun, C. H.; Qiao, S. Z.; Zou, J.; Liu, G.; Smith, S. C.; Cheng, H. M.; Lu, G. Q. *Nature* **2008**, *453*, 638–641.

(32) Lawton, S. L.; Leonowicz, M. E.; Partridge, R. D.; Chu, P.; Rubin, M. K. *Microporous Mesoporous Mater.* **1998**, *23*, 109–117.

(33) Corma, A.; Martínez-Soria, V.; Schnoeveld, E. *J. Catal.* **2000**, *192*, 163–173.

(34) Degnan, T. F. *J. Catal.* **2003**, *216*, 32–46.

(35) Derouane, E. G.; Andre, J.-M.; Lucas, A. A. *J. Catal.* **1988**, *110*, 58–73.

(36) Sastre, G.; Corma, A. *J. Mol. Catal. A: Chem.* **2009**, *305*, 3–7.